Methods for Determining Characteristics of Acoustic Waves in Rocket Motors

H. B. MATHES* AND E. W. PRICE†
Naval Weapons Center, China Lake, Calif.

Combustion instability in rocket motors is associated with gas oscillations in one or more standing acoustic wave modes within the motor. Knowledge of the structure of these modes is needed for understanding of firing data, proper instrumentation of the motor, and for stability calculations. Two methods of determining standing acoustic wave frequency and mode structure are discussed: one involves use of acoustic models, and the other consists of solutions to a finite-element program by high-speed digital computer. Acoustic model results are compared with computer solutions and with motor firing data.

I. Introduction

MANY rocket motors have vibrations associated with burning of the propellant which remain a characteristic of the motor through development and into its production and service life. The Poseidon second stage motor is no exception, typically showing vibrations at nine different frequencies which exist during some portion of the first ten seconds of motor operation.[1] To date, the vibrations are not known to have prevented completion of the missile's mission but there is concern that minor changes in one or more parameters which occasionally occur during a motor's production history may increase the vibration level and consequently interfere with some vital function such as guidance or thrust termination. Therefore, a series of investigations was initiated to: a) determine the cause and characteristics of the vibrations, and b) monitor propellant combustion characteristics and vibrations during static and flight tests of motors throughout production to detect increases in vibration levels should they occur. This paper describes methods used for determining the acoustic characteristics of the interior of the motor.

II. Sub-Scale Model Experiments

Although several possible causes for the observed vibrations were suggested, it seemed that the most likely cause was combustion-driven acoustic waves in the motor. A series of experiments, therefore, was designed to determine the frequencies and structural characteristics of standing acoustic waves in the motor. Many of the instrumentation and experimental techniques used in this work were adapted from earlier work relating to determination of acoustic losses in sub-scale rocket motors.[2-4] In the present case, however, no provisions for gas flow in the model were made.

Drawings obtained from the motor manufacturer which showed internal details of the motor were used to build three models which were made to $\frac{1}{4}$ full-scale and for propellant grain surfaces representing the grain as cast (zero time) and for 2.5 and 7.0 sec of time after ignition. The models were cast with an aluminum-filled epoxy resin. A head-end closure with $\frac{1}{4}$-scale igniter and an aft end closure carrying a $\frac{1}{4}$-scale nozzle were fabricated. End closure attachments were arranged so they could be used on all three model castings. Holes were bored through the sides of each of the models and through the head-end and nozzle closures to allow access for acoustic drivers and microphones to the model interior. Internal geometry of a model and location of access holes are shown in Fig. 1. Hole location is specified by a letter/number which indicates the axial and circumferential positions, respectively. The head closure was constructed so that the central portion could be rotated. The rotating portion was perforated with two holes so that microphones could be inserted. One of the holes which located a microphone at the edge of the simulated propellant was off center, approximately the same relative distance off-axis as the pressure transducers on the full-scale motor. The other hole was

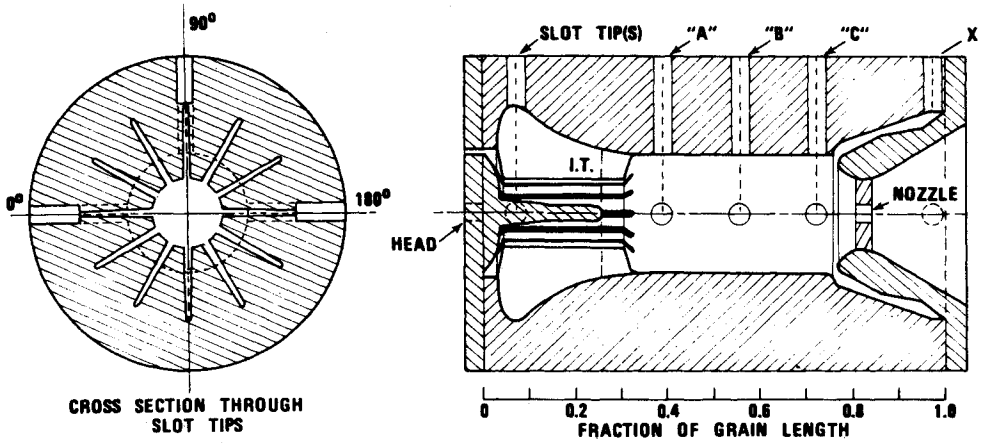

Fig. 1 Sections through an acoustic model showing details of internal geometry and locations of hole in the model for driver and microphone access.

Presented as Paper 74-196 at the AIAA 12th Aerospace Sciences Meeting, Washington D.C., January 30–February 1, 1974; submitted April 15, 1974; revision received August 29, 1974.
Index categories: Combustion Stability, Ignition and Detonation; Rocket Engine Testing; Wave Motion and Sloshing.
* Physicist, Aerothermochemistry Division, Research Department, Naval Weapons Center, China Lake, Calif.
† Head, Aerothermochemistry Division, Research Department, Naval Weapons Center, China Lake, Calif. Fellow AIAA.

on-axis and permitted a specially designed $\frac{1}{2}$-in. variable capacitance microphone to be inserted and to be moved along the interior of the model.

Two $\frac{1}{4}$-in. variable capacitance microphones were used to detect acoustic oscillations. A small acoustic generator originally used in a sound-powered communication system was used as the driver. The driver and $\frac{1}{4}$-in. microphones were adapted so they could be used interchangeably at any of the access holes in the model. A number of blank plugs were also made which could be used to block off all unused holes, thus preventing unwanted leakage of acoustic energy from the model. All inserts were equipped with O-rings for added assurance against acoustic leakage. A nozzle closure plate was fabricated which could be placed in the throat. It too was fitted with O-rings so that the closure could be tightly sealed. The throat closure plate was drilled with an on-axis hole which was adapted so it could accept either the standard microphone/driver insert or the specially built $\frac{1}{2}$-in. microphone extension which could be slid through an O-ring seal in the plate and moved along the model axis.

Two important factors in this type of acoustic testing are to isolate the driver from the cavity and to provide a means of applying a constant driver amplitude over a wide frequency range. Driver cavity isolation was achieved by placing an acoustic resistance between the driver and the cavity. The resistance consists of a tightly packed bundle of small metal rods which fill the channel between the driver and the model interior. Measurements show that the resistance is sufficient to effectively prevent acoustic pressure in the model cavity from appearing in the driver section. This feature is important because the acoustic amplitude in the driver section is fed back to a compensating circuit in the variable frequency oscillator which is used to provide output signal adjustment so that the driver operates at nearly constant amplitude over the range of test frequencies. Use of the drive compensating ("compressor") circuit results in a maximum driver amplitude deviation of 4.2 db from 200 Hz to 5kHz. Driver deviation without compensation was 69 db over the same range of frequencies.

Test procedure consisted of making a "frequency sweep run" using the oscillator drive unit to provide for a continuous variation of frequency. Data from sweep runs were recorded on a dual pen X-Y plotter which plotted acoustic amplitude as a function of frequency, resulting in an acoustic spectrogram. On completion of a sweep run, the oscillator drive unit was disengaged and the oscillator was manually tuned to each peak of interest in the spectrogram. When tuned, the frequency of the resonant peak was read from a digital frequency meter. The instrumentation system for this type of test is shown in Fig. 2.

After completion of procedures for recording the acoustic spectrogram and for determining the resonant frequencies, the instrumentation system was rearranged to permit recording of axial pressure distribution for each peak in the spectrogram. Axial wave structural characteristics were determined by tuning the frequency to the frequency of interest and moving a microphone along the model axis. The microphone could be used to

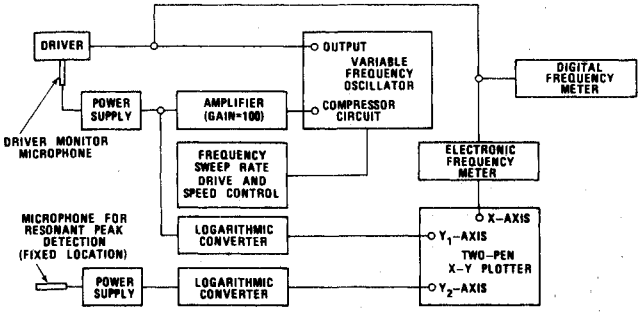

Fig. 2 Instrumentation for obtaining acoustic spectrograms and for determination of resonant frequencies.

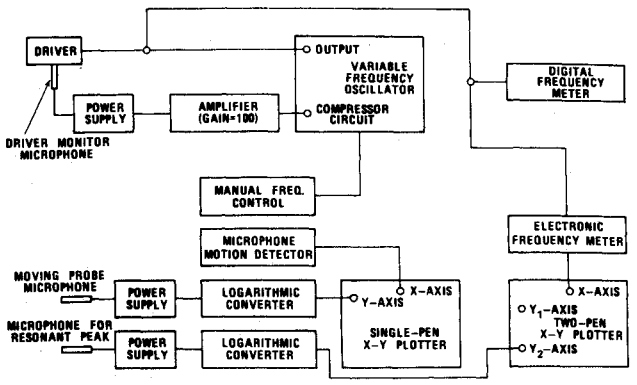

Fig. 3 Instrumentation arrangement used to obtain acoustic pressure distributions.

measure on the model centerline or, by using a 90° angle head, to measure the pressure distribution in a line parallel to the axis of symmetry, giving a longitudinal pressure distribution near the model wall. The instrumentation system provided means for detecting the position of the moving probe and for continuously recording on an X-Y plotter the acoustic pressure as a function of position in the model. The instrumentation used in this phase of testing is shown in Fig. 3.

Determination of circumferential pressure distribution followed generally the procedure described for axial distribution except that the microphone was fitted with a 90° offset head and the microphone was rotated. A provision for detecting the degree of rotation of the head permitted a continuous recording of pressure distribution to be provided by an X-Y plotter. An instrumentation arrangement similar to that shown in Fig. 3 was used for this type of measurement.

No provision was made to record radial pressure distribution or the distribution in the nozzle annulus. Such measurements, when needed, were made with a 2mm probe tube attached to the end of a microphone, the whole assembly being moved by hand and the probe position and microphone output noted by handwritten data.

III. Computer Determination of Modes

Another method for determining the characteristics of acoustic waves in rocket motors involves a numerical analysis program and a large scale, high-speed digital computer. This approach relies on computer simulation of the acoustic medium and cavity boundaries rather than on direct measurement of physical phenomena. The NASTRAN (*NASA STR*uctural *AN*alysis) program, one of several programs which have been used to simulate the characteristics of acoustic waves in rocket motors, was originally developed for dynamic analysis of complicated structures. It has been modified, in conjunction with work at another laboratory, for simulating the acoustics of a cavity with complicated shape, the details of which are treated in Ref. 5. Preparation of a problem for solution includes reducing the dimensions of the cavity being treated from three to two and dividing the cavity into a number of elements. Each element has a "mass" and is connected by "springs" to adjoining elements and to the cavity boundary to form a spring-mass equivalent of the gas in the motor. The computer program provides for perturbing the system, for determining the standing wave frequencies of the system, and for providing a graphical plot of relative wave amplitude and phase as functions of position in the cavity for each frequency.

Input data for the Poseidon second-stage motor were submitted for comparing the NASTRAN acoustic program predictions with measurement in the $\frac{1}{4}$-scale model. Solutions were obtained for the zero-time and 7-second configurations described above and the results were compared with the $\frac{1}{4}$-scale model results.

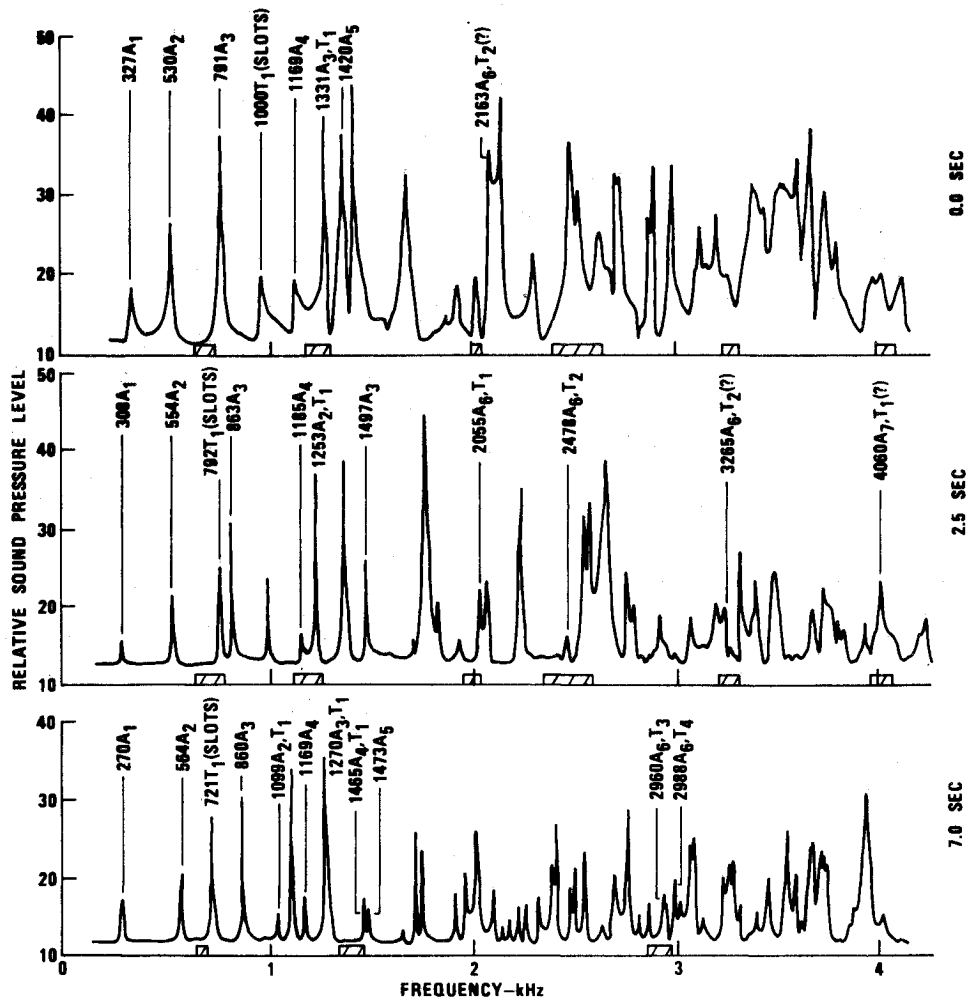

Fig. 4 Acoustic spectrograms from the 1/4-scale models for three burn times.

Comparison of computer-based and experimentally determined frequencies is made in Table 1. Several frequencies predicted by the computer were not initially detected in the model. Further investigation revealed that these particular frequencies represented oscillations that the computer indicated would be of relatively high amplitude in the nozzle annulus but weak in the central and head-end portions of the cavity. Waves of such structure were later verified experimentally in tests instrumented specifically for the purpose.

Table 1 Comparison of calculated (NASTRAN) and 1/4-scale experimentally determined frequencies (adapted from Table 4 in Ref. 5)

Wave Designation[5]		0.0 sec		7.0 sec	
n	Mode	NASTRAN	Experiment	NASTRAN	Experiment
0	1	319.0	327	266.3	265
	2	530.2	530	557.6	566
	3	790.8	791	854.2	856
	4	1168.9	1169	1176.1	1171
	5	1454.1	1420	1505.0	1505
	6	1652.2	1751	1639.4	1639[a,b]
1	1	686.5	...	606.5	589[a]
	2	1079.6	1000	685.5	713
	3	1380.2	1332	1104.8	1109
	4	1506.6	1478	1280.8	1276
	5	1730.9	...	1489.9	1461[a,c]
	6	1838.6	...	1750.9	1721

[a] "Found" in model after reviewing computer results.
[b] There is also a strong wave in the nozzle annulus at 1652 Hz.
[c] There is also a wave of similar strength at 1473 Hz.

Comparison of acoustic model results with motor firing data is shown in Fig. 7. Here the differences between acoustic prediction from model experiments or from the finite element computer program are apparent; motor frequencies above 1000 Hz do not follow the time-frequency trend of a particular acoustic wave structure. Model data is represented by solid circles and dashed lines while shaded bars indicate baseline vibration data from motor firings.

IV. Results

Preliminary tests were conducted in the models with the nozzle throat open and with it closed. Those tests showed that the axial wave frequencies in the models more closely corresponded to motor frequencies when the throat was closed, indicating that axial acoustic waves in the motor are structured for a "closed-closed" cavity rather than a "closed-open" one. Therefore, most of the testing and all of the results discussed below are with the nozzle throat closed.

When the procedures described in the previous section were completed, the acoustic wave frequencies and structural characteristics for the three models could be described. Acoustic spectrograms from the three models with annotations appear in Fig. 4. Frequency and wave structure are indicated for selected resonant peaks in Fig. 4. All three spectrograms in that figure were obtained with the driver located at A – 0° and with the microphone placed in an offset hole in the head closure at 180°. Shaded bars in the figure indicate portions of the spectrum in which motor vibrations are detected. Typical axial and tangential pressure distributions appear in Fig. 5. The longitudinal distributions for 265, 566, and 856 Hz were determined with an offset head measuring $\frac{1}{4}$-in. from the wall in the central (cylindrical) section. Dashed lines represent pressures determined by a

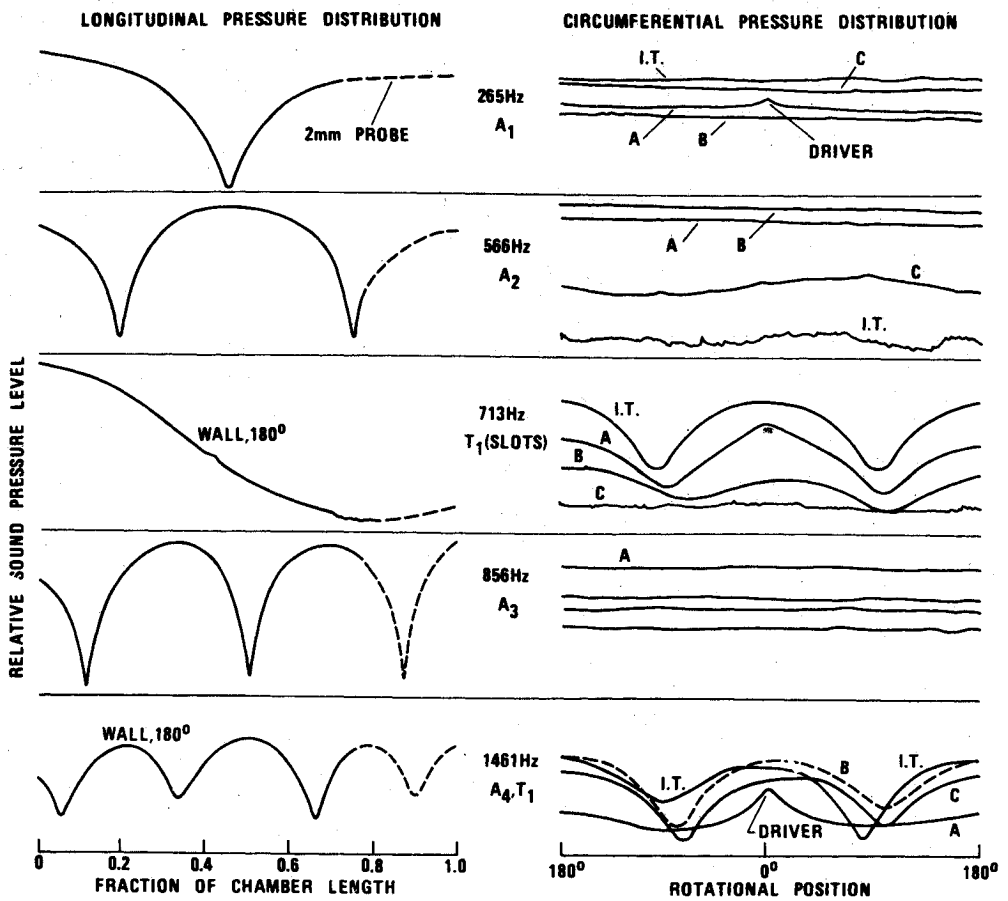

Fig. 5 Longitudinal and circumferential pressure distributions of selected peaks in the 7-sec model.

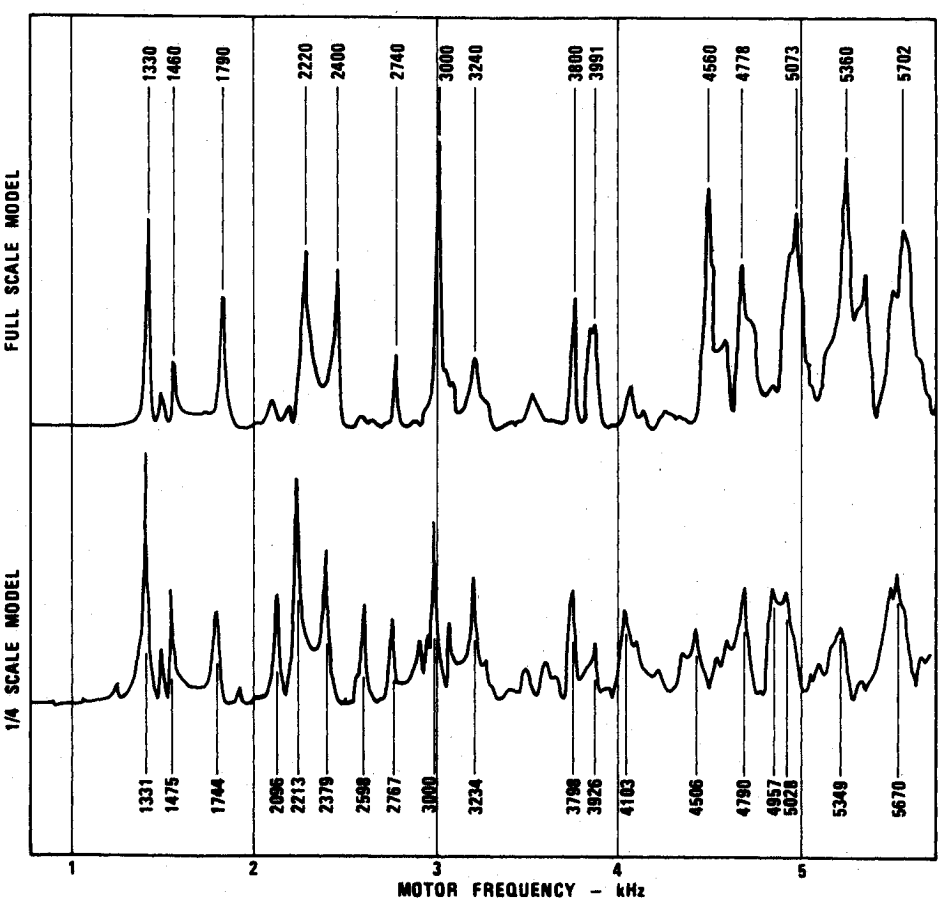

Fig. 6 Comparison of full-scale and 1/4-scale acoustic model results.

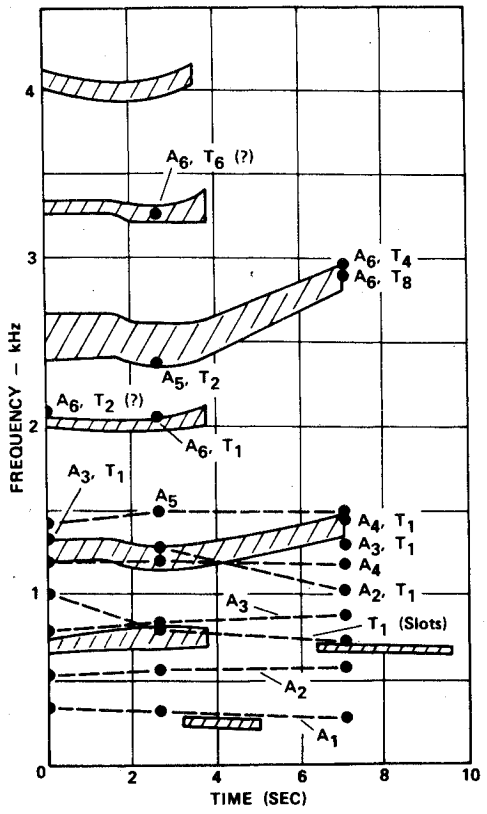

Fig. 7 Comparison of 1/4-scale model results with motor vibration data.

2-mm microphone probe moved by hand in the nozzle annulus. The circumferential distributions were all determined by the offset head described above. Axial locations of circumferential measurements are identified by letters indicating position (see Fig. 1). Some of the distributions show a disturbance created by the driver which was located at A – 0°.

As would be expected for complicated geometries, the wave frequencies and structural characteristics did not follow a simple pattern. However, a system derived from classical right circular cylindrical acoustics was used to identify the various structural characteristics. For axial waves, the number of nodes detected between the head-end of the cavity and the aft terminus of the annular space around the nozzle was the "wave number" for the axial component at each frequency for which an axial distribution was detected. For waves showing a tangential distribution, the number of nodes from 0° to 180° was the wave number. Radial structure was denoted by the number of nodes between the axis of symmetry and the wall. Letter designations used for structural characterization are: A for axial, T for tangential, and R for radial. Waves showing a combination of structures are denoted by an appropriate combination of symbols; for example, a resonant peak showing a combination of axial and tangential structural characteristics would be detoned as A2, T3, to describe a second axial wave structure in combination with a third tangential.

Similar tests were conducted in the motor manufacturer's plant using a full-scale inert loaded motor with internal geometry representing conditions at ignition (zero time). Questions concerning the validity of sub-scale tests were raised during the course of the investigation. The degree to which sub-scale and full-scale models provide similar results is indicated in Fig. 6 which compares swept frequency runs in both zero-time configurations using similar driver and detector locations. Differences between results are minor indicating that size per se is not an important factor in determining acoustic wave characteristics. It should be noted, however, that there are practical size limits on both the large and small end of the scale; larger sizes are not only more expensive to build but may result in some of the lower frequencies being too low for one driver to excite; small scale models are relatively inexpensive to make and operate but may make acoustic probe measurements (particularly traveling probes) difficult to achieve without affecting the cavity's wave characteristics.

V. Discussions and Conclusions

One of the remarkable features of the acoustic data is the large number of resonant peaks observed. As many as 55 peaks can be seen in one configuration over the 200 Hz to 4 kHz frequency range. Many of the peaks are weak and are probably of little interest so far as explaining motor behavior is concerned. Many of the major peaks occurring in the model appear at or near frequencies which have been seen in the motor.

Most of the resonant peaks above 1 kHz have the structure of combination modes—all that have been clearly identified in the $\frac{1}{4}$-scale models are combinations of tangential and axial oscillations.

Comparison of experimental results with computer calculations indicates that the computer does a reasonably good job of predicting the acoustic characteristics of a cavity with complicated geometry. However, there are limitations on the calculations, and the extent to which the computer solutions can simulate all the results obtained in the experiment have not been determined. This naturally raises the question of how far to go in such an investigation. The answer certainly depends on the approach. In the present case, the acoustics investigation was a follow-on to phenomena seen in the motor, which provided a valuable guide. In a case where a motor geometry is to be characterized without benefit of firing data, a more extensive set of measurements or of calculations would probably be justified.

An explanation of the presence or absence of oscillations in the motor requires not only knowledge of the various frequencies but a consideration of the stability of each of the possible standing waves in the motor. Such considerations are beyond the scope of this discussion but are necessary to explain, in the present case, the motor's preference for exciting certain frequencies (above 1000 Hz) rather than following the frequency-time characteristic of any of the standing waves. However, calculations to predict what modes will be excited requires prior knowledge of mode structure, by either computer or experimental studies such as these studied here.

Acoustic modeling, either of full-sub-scale versions of the motor or by computer analysis, offers the means for determining the acoustic characteristics of a rocket motor of complicated internal geometry. The particular method used to determine acoustic characteristics will depend on the relative cost of experiments against the cost of treatment by computer, as well as by availability of equipment. The results of such analysis may provide a useful guide for study of motor instability.

References

[1] Pendleton, L. R., "Sinusoidal Vibration of Poseidon Solid Propellant Motors," *Shock and Vibration Bulletin*, Vol. 3, Jan. 1972, Naval Research Laboratory, Washington, D.C., p. 89.

[2] Mathes, H. B., "Effect of Geometrical Variables on Losses in Motors as Determined by Cold-Flow Model Testing," *Proceedings of the 1st Interagency Chemical Rocket Propulsion Group Combustion Instability Conference*, Vol. 1, Nov. 1964, p. 443.

[3] Buffum, F. G., Dehority, G. L., Slates, R., and Price, E. W., "Acoustic Attenuation Experiments on Sunscale Cold Flow Rocket Motors," *AIAA Journal*, Vol. 5, No. 2, Feb. 1967, pp. 272–280.

[4] Slates, R. O., Buffum, F. G., and Dehority, G. L., "Acoustic Attenuation in Resonant Model-Rocket Motors," *Proceedings of the ICRPG/AIAA Second Solid Propulsion Conference*, 1967, pp. 173–180.

[5] Herting, D. N., Joseph, J. A., Kuusinen, L. R., and MacNeal, R. H., "Acoustic Analysis of Solid Rocket Motor Cavities by a Finite Element Method," AFRPL-TR-71-96 (MSC Rept. MS116-3), no date.